Cell Tissue Bank (2024) 25:721–734
https://doi.org/10.1007/s10561-024-10136-1

FULL LENGTH PAPER

Decellularized kidney capsule as a three-dimensional scaffold for tissue regeneration

Mohammad Rasool Khazaei · Rawa Ibrahim · Rayan Faris · Azam Bozorgi · Mozafar Khazaei · Leila Rezakhani

Received: 19 March 2024 / Accepted: 9 April 2024 / Published online: 26 April 2024

Abstract Tissue regeneration is thought to have considerable promise with the use of scaffolds designed for tissue engineering. Although polymer-based scaffolds for tissue engineering have been used extensively and developed quickly, their ability to mimic the in-vivo milieu, overcome immunogenicity, and have comparable mechanical or biochemical properties has limited their capability for repair. Fortunately, there is a compelling method to get around these challenges thanks to the development of extracellular matrix (ECM) scaffolds made from decellularized tissues. We used ECM decellularized sheep kidney capsule tissue in our research. Using detergents such as Triton-X100 and sodium dodecyl sulfate (SDS), these scaffolds were decellularized. DNA content, histology, mechanical properties analysis, attenuated total reflection Fourier transform infrared spectroscopy (ATR-FTIR), biocompatibility, hemocompatibility and scanning electron microscope (SEM) imaging were measured. The results showed that the three-dimensional (3D) structure of the ECM remained largely intact. The scaffolds mentioned above had several hydrophilic properties. The best biocompatibility and blood compatibility properties were reported in the SDS method of 0.5%. The best decellularization scaffold was introduced with 0.5% SDS. Therefore, it can be proposed as a scaffold that has ECM like natural tissue, for tissue engineering applications.

Keywords Kidney capsule · Decellularization · Scaffold · Tissue regeneration · Tissue engineering

M. R. Khazaei · A. Bozorgi · M. Khazaei · L. Rezakhani
Fertility and Infertility Research Center, Health Technology Institute, Kermanshah University of Medical Sciences, Kermanshah, Iran

M. R. Khazaei · A. Bozorgi · M. Khazaei · L. Rezakhani (✉)
Department of Tissue Engineering, School of Medicine, Kermanshah University of Medical Sciences, Kermanshah, Iran
e-mail: leila_rezakhani@yahoo.com; Leila.rezakhani@kums.ac.ir

R. Ibrahim · R. Faris
Student Research Committee, Kermanshah University of Medical Sciences, Kermanshah, Iran

Introduction

In order to create tissues and organs that can assist address the shortage of donor organs, tissue engineering, a branch of regenerative medicine, uses biological science and engineering. In order to restore the normal function of tissues, tissue engineering places cells into desired biological structures within a predetermined framework (Neishabouri et al. 2022). Cells, signaling factors, and scaffolds are the three main components of this process. Scaffolds are a vital part of tissue engineering because they permit the supply of the necessary growth factors for tissue regeneration while also offering mechanical stability and structural

support for foreign cell adhesion and proliferation (Zhang et al. 2022). Scaffolds can be built from synthetic biomaterials or natural tissues that have been taken from human or animal sources. Natural scaffolds provide biological properties that better match the normal tissue milieu, encouraging biocompatibility, degradability, and suitable cellular interactions (Sharifi et al. 2022; Ehterami et al. 2021).

It is difficult to reproduce the various ECM compositions and complexity seen in different tissues. Therefore, appropriate biomaterial platforms for the healing of various tissues may be developed using tissue decellularization procedures. In a decellularized tissue, the cellular components are eliminated yet the tissue-specific ECM microenvironment is kept. As a result, it can serve as a functional tissue-specific scaffold with desired qualities including biocompatibility and low immunogenicity (Lee et al. 2022, 2018). Both preclinical animal investigations and human therapeutic applications have had success using biological scaffolds made from decellularized tissues and organs. The ECM scaffold's mechanical properties and tissue structure are both impacted by decellularization techniques (Prasertsung et al. 2008; Kim et al. 2021). In this study, for the first time, the kidney capsule was decellularized with different methods and analyzed for tissue engineering.

Methods and materials

Preparation of kidney capsule tissues

One of the dietary sources is sheep meat. Kidneys were removed from a two-year-old male Sanjabi breed sheep sacrificed at the Kermanshah, Iran animal abattoir in Iran. The kidney capsule was gently separated from the tissue surface and placed in phosphate-buffered saline (PBS) (Sigma Aldrich) containing 2% penicillin–streptomycin (P/S) antibiotic for further processing.

Decellularization process

The kidney capsule was divided into tiny (2×2 cm^2) fragments. Three different techniques were utilized in this investigation to decellularize the tissue: 0.5% sodium dodecyl sulfate (SDS) (Sigma Aldrich), 1% SDS, and 0.1% SDS-0.5% Triton-X100 (Sigma Aldrich). The tissues in the decellularization procedures were immersed in the appropriate detergents and agitated for 24 h at 80 revolutions per minute (rpm). The tissues were then cleaned again for 24 h at an 80 rpm speed in distilled water. The samples were submerged in 70% ethanol for 15 min then each side of the scaffold was subjected to UV light for 15 min to finish sterilizing it.

DNA content

Using a kit from the Iranian company Sinaclon, the residual DNA content in the decellularized kidney capsules (DkCs) was measured. DkCs (30 mg) were mixed with protease buffer (100 µl) and protease (5 µl) and then maintained at 55 °C for 4 h. 100 ml of the sample was combined with 400 ml of the lysis solution and 300 ml of the precipitation solution before being centrifuged at 12,000 g for 10 min. The pellet is centrifuged for 30 s at 12,000 g while being suspended in a solvent buffer (50 µl). A NanoDrop spectrophotometer (BioTeK) was used to quantify the supernatant's DNA concentration (Khazaei et al. 2023a, b).

Biocompatibility evaluation (MTT assay)

The ISO 10993-5 standard was used to conduct an indirect assessment for DKCs biocompatibility. For 24 h, sterilized DKCs was incubated in a Dulbecco's Modified Eagle's medium (DMEM–Sigma) culture media. To test biocompatibility at 48 and 72 h using the MTT assay, the medium condition was collected and added to cultivated adipose mesenchymal stem cells (AMSCs) from the Pasteur Institute in Iran (1×10^4 in each well of 96 plates). Following the appropriate time periods, 20 µl of the MTT solution (5 mg/ml concentration, Sigma-Aldrich) was transferred to the cells, and the plate was incubated for 4 h. The purple formazan crystals were then dissolved by adding 100 µl of dimethyl sulfoxide (DMSO) from Sigma-Aldrich to the wells containing the cells after the MTT solution had been withdrawn (Guarnieri et al. 2022). Finally, an ELISA reader (Stat Fax 2100, USA) was used to measure the quantity of light absorption. The results were calculated with the following formula: Cell biocompatibility (%) = Sample OD/Control OD × 100.

Histology analysis

The samples were fixed, dried, and paraffin-embedded before being evaluated histologically for both native kidney capsule (NKC) and DKCs. A microtome was then used to create slices with a diameter of 5 microns. Hematoxylin–eosin (H&E), Masson trichrome (MT), and Alcian blue (AB) staining were then performed on these slices. An optical microscope was used for tests to see the nucleus, collagen, and glycosaminoglycan (GAG) in the DKCs (Alizadeh et al. 2020).

Hemocompatibility evaluation (hemolysis test)

2 ml of PBS was poured to each of the DKC pieces, which were individually cut into 3 × 3 mm squares. After that, they were incubated at 37 °C for 30 min. 2 ml of distilled water was administered to the positive control group, whereas 2 ml of PBS was given to the negative control group. Each sample tube received 20 µl of fresh blood with anticoagulants, which was then incubated at 37 °C for an hour. The tubes were then centrifuged for 10 min at 1500 rpm. Using an ELISA reader (Stat Fax 2100, USA), the optical absorbance was determined at 545 nm after the supernatant was removed (Ehterami et al. 2022). The degree of hemolysis (HD) was estimated using the formula below: Dn: sample, D0: negative control, D1: positive control. $HD\ (\%) = [(Dn - D0)/(D1 - D0)] \times 100$.

Blood clotting index (BCI)

To learn more about the scaffolds' ability to act as hemostatic, whole blood clotting research was conducted. The DKCs were put in Petri dishes that had been warmed at 37 °C for 5 min to determine the hemostatic potential of the material, which increased with a decreased blood coagulation index. 300 µl of fresh blood containing anticoagulant was placed over the DKCs, and 25 µl of 0.2 M CaCl2 was added to start the coagulation process. A spectrophotometer was used to measure the absorbance of the released hemoglobin at a wavelength of 542 nm after hemolyzing the red blood cells (RBC) with 15 ml of distilled water for 10 min. The control group does not have a scaffold (Sharma et al. 2019). The following formula was used to get the blood coagulation index: %BCI = OD sample/OD control × 100.

Mechanical test

The Santam st-1 device (Iran) was employed to research the mechanical characteristics of scaffolds. The device's clamp was inserted between NKC and DKCs and the device's tensile strength was measured. Using the following formulae, stress, strain, and Young's modulus were determined. Once the samples were broken down the test was terminated, and the load cell's output was 1000 Newton (N) (Khazaei et al. 2023b). F = force, A° = cross-section, ΔL = change in length, L° = initial length, ΔS = change in stress (Stress) $S = F/A^{\circ}$, (Strain) $E = \Delta L/L^{\circ}$, (Young's modulus) $E = \Delta S/\Delta e$.

Cell morphology and attachment (SEM)

The ultrastructural study of both NKC and DKCs was done using the scanning electron microscope (SEM) (Philips Company, the Netherlands). Initially, the samples were subjected to a fixative solution containing 2.5% glutaraldehyde (Sigma Aldrich) for 24 h. Ascending values of ethanol were used to dehydrate the samples. The specimens were coated with gold–palladium after drying to aid in microscopic examination. A total of 1×10^4 AMSCs were cultured on DKCs to study cell adhesion on the scaffold. The cells were then treated to 72 h of incubation. Using a 2.5% glutaraldehyde solution, the samples were fixed (Ehterami et al. 2021).

Contact angle

Deionized water was dropped onto the scaffold surfaces using a syringe with a 27 G needle; an image of the drop was taken on the scaffold; and the contact angles were calculated according to the drop shape with Image J software (Gao et al. 2017).

Water retention capacity (WRC)

The dry tissues were weighed, submerged in PBS for a period to determine the scaffolds' ability to retain water, and then incubated for 24 h at 37 °C. After being placed in a centrifuge tube with

filter paper underneath, the scaffolds were spun at 500 rpm for three minutes (Chandika et al. 2015). The scaffolds were then weighed once again, and the formula following was used. Ws: the weight of the swollen scaffold, Wi: weight of the dry scaffolds WR (%) = (Ws − Wi)/Wi × 100.

In order to test the contact angle and WRC, the scaffolds were dehydrated in ascending ethanol solutions (40, 50, 60, 70, 80, 90 and 100%), then frozen at − 70 °C for 6 h. Then they freeze-dried at − 50 °C for 12 h (Christ Alpha 2–4 LDplus) (Wang et al. 2018).

Attenuated total reflection Fourier transform infrared spectroscopy (ATR-FTIR) analysis

Investigation of the bonds formed, the identification of functional groups, and the molecular structure of the scaffolds were evaluated using FTIR spectroscopy. Infrared spectra of the NKC and DKCs were recorded using Nicolet Is10 (Thermo Fisher Scientific, USA) equipped with ATR mode over the range of 500–4000 cm^{-1} at a resolution of 4 cm^{-1} averaged over 64 scans (Sizeland et al. 2018).

Statistical analysis

Each outcome in this study had its average and standard deviation determined, and every test had at least three repetitions. The one-way ANOVA and Tukey's post hoc test were used to analyze the data using GraphPad Prism software (version 8). The significance value was established at $P \leq 0.05$.

Results

DNA content and biocompatibility

DNA content was checked to confirm decellularization in DKCs samples and compared with NKC. Significant difference ($P < 0.001$) in DNA concentration between NKC (514.23 ± 0.32 ng/mg) and DKCs (0.5% SDS: 48.74 ± 0.62 ng/mg, 1% SDS: 33.62 ± 0.89 and 0.1% SDS-0.5% Triton: 65.65 ± 0.77 ng/mg mg) was observed. A decrease in DNA content after decellularization was observed in all methods (Fig. 1A). The MTT test was carried out to determine the cytotoxicity of the scaffolds with AMSC cells at 48 and 72 h. A percentage of the appropriate main cell population is used to express

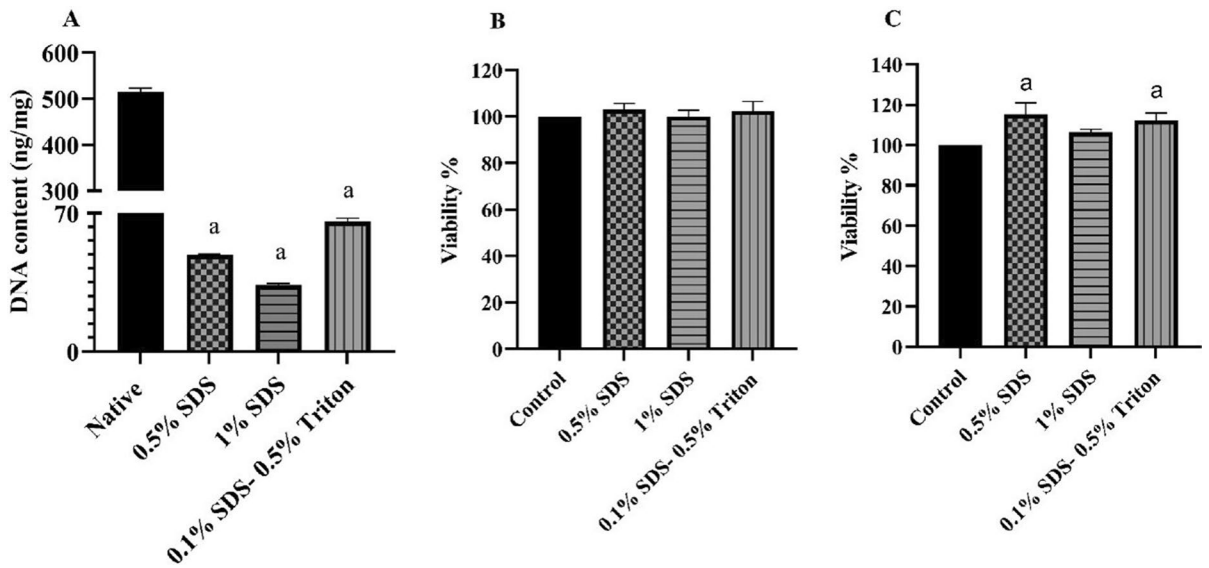

Fig. 1 **A** DNA content in DKCs samples showed a significant difference with the NKC sample, **B** MTT test in 48 h and **C** MTT test in 72 h, cytotoxicity evaluation after 48 and 72 h shows high cell proliferation for all groups. All experimental groups reported cell viability above 100%, a: Significant compared to the control group, the data presented are mean ± SD, n = 3

the findings of the cell proliferation evaluation. In all experimental groups, cell viability was greater than 100%, as seen in Fig. 1B, C. In comparison to the other two groups, the 1% SDS group reported a lower survival percentage. Within 48 h, there was no significant difference between the control group and the other test groups. 0.5% SDS and 0.1% SDS-0.5% Triton groups, however, were significantly different from the control group after 72 h. Data revealed that the scaffolds were biocompatible and that none of the study techniques' decellularization procedures did not cause toxicity.

Histology

Histological staining of NKC and DKCs samples can be seen in Fig. 2. The native tissues had excellent cellular organization, extracellular matrix density, a collagen network, and GAG. The nuclei are clearly visible in the tissue. With the 0.5% SDS procedure, the

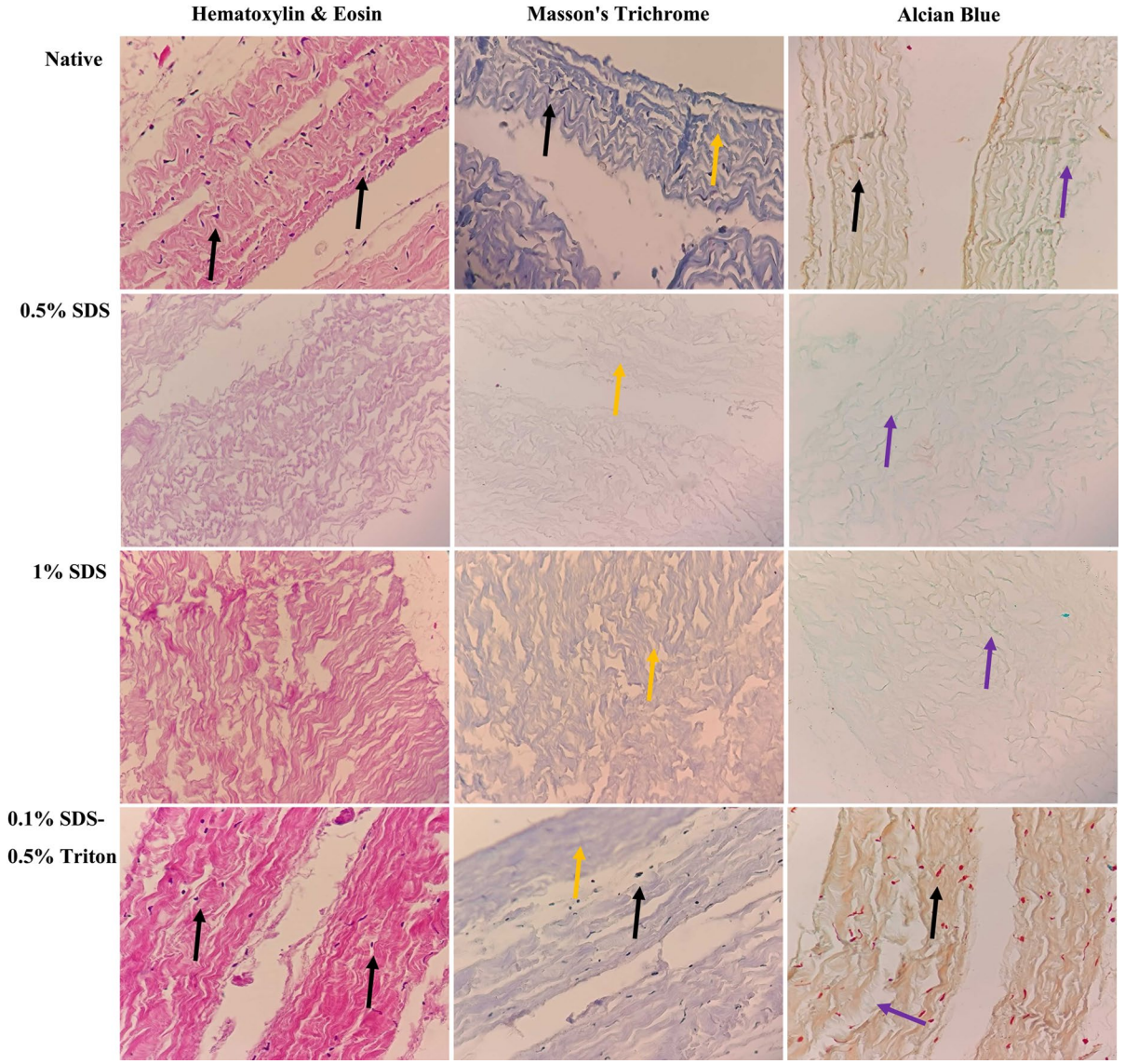

Fig. 2 Histological staining in NKC and DKCs tissues. magnification 200×. Black arrows show nuclei, orange arrows show collagen structure, and purple arrows show GAG in native tissue and decellularized tissues

structural order and morphological organization have been mostly maintained. While the nuclei are entirely absent from the tissue, collagen, and GAG structure are still there. The tissue structure is partially destroyed, and all the nuclei are lost during the 1% SDS process. The tissue morphology was adequately retained using the 0.1% SDS-0.5% Triton technique, however, the cells could not be entirely separated from the matrix. In terms of network order and cell removal, the decellularization sample obtained using the 0.5% SDS procedure exhibited maximum efficiency.

Hemolysis test and BCI

The hemolysis test results are displayed in Fig. 3A. A significant difference was seen in the hemocompatibility of all tissues decellularized using different procedures compared to the positive control group. The percentage of hemolysis was reported in the 1% SDS method (2.58%), while in other methods this value was less than 1%. A lower BCI value indicates a stronger homeostatic potential of the material. 0.5% SDS showed significantly better homeostatic ability (20.33%) compared to the 1%SDS (38.66%) and 0.1% SDS-0.5% Triton (23.33) (Fig. 3B).

Mechanical test

The mechanical test showed that the native tissue has Young's modulus equal to 50.06 ± 1.23 MPa, which was higher compared to all the samples. In protocol 0.5% SDS and 1% SDS, Young's modulus was reported as 32.97 ± 1.67 and 31.56 ± 1.45, respectively, which had a strain close to that of the native sample. In the 0.1% SDS-0.5% Triton protocol, a higher strain was obtained than all the samples, and Young's modulus was reported as 42.01 ± 1.39. (Fig. 4).

SEM

SEM images (Fig. 5) showed that the ECM structure is coherent in the NKC. In the 0.5% SDS decellularization method, the fibers are broken up to a certain extent, and cell adhesion has occurred well so that the cells have covered the surface of the scaffold. In the 1% SDS method, collagen fibers are separated more than other groups. Cell adhesion was also observed in this method and the 0.1% SDS-0.5% Triton method.

Contact angle and WRC

The contact angle test was performed to measure the hydrophilicity of the scaffold surface (Fig. 6A). The degree of hydrophilicity of the scaffolds with different detergents is different from each other and the contact angle in the decellularization method with 1% SDS (30.07 ± 0.24) was reported to be higher than 0.5% SDS (15.03 ± 0.34) and 0.1% SDS-0.5% Triton (11.84 ± 0.31). With the decrease in SDS concentration, the degree of hydrophilicity has increased. The water retention qualities play a crucial role in stabilizing the form and size of the scaffolds and serving as important markers of physiological fluid absorption. Figure 6B depicts the WRC. The water retention by the 0.5% SDS, 1%SDS, and 0.1% SDS-0.5% Triton scaffolds was 263.66 ± 2.02, 295 ± 2.43, and 205.33 ± 1.98, respectively.

ATR-FTIR

ATR-FTIR spectroscopy of NKC and DKCs was performed to analyze the structural changes in collagen after decellularization. ATR-FTIR spectra of NKC and DKCs are exhibited in Fig. 7. Native tissue mainly exhibited five absorption peaks at 3291 cm^{-1}, 2921 cm^{-1}, 1630 cm^{-1}, 1540 cm^{-1}, and 1235 cm^{-1}, corresponding to amide A, amide B, amide I, amide II, and amide III, respectively. These areas are shown in Fig. 7 with dashed dots for each of the decellularization methods. Several peaks were found in the 1000–1100 cm^{-1} range in each of the NKC and, DKCs. However, the spectral peak due to C–O– stretching vibration which is specific for keratan sulfate (GAG) appeared at 1080 cm^{-1}, NKC. Thus, the result indicated relatively high GAG content in 0.5% SDS DKC as compared to other decellularized methods.

Discussion

The requirement for transplant patients cannot be met by the amount of organ donors; thus, research in the fields of tissue engineering and regenerative medicine aims to offer substitute therapeutic approaches

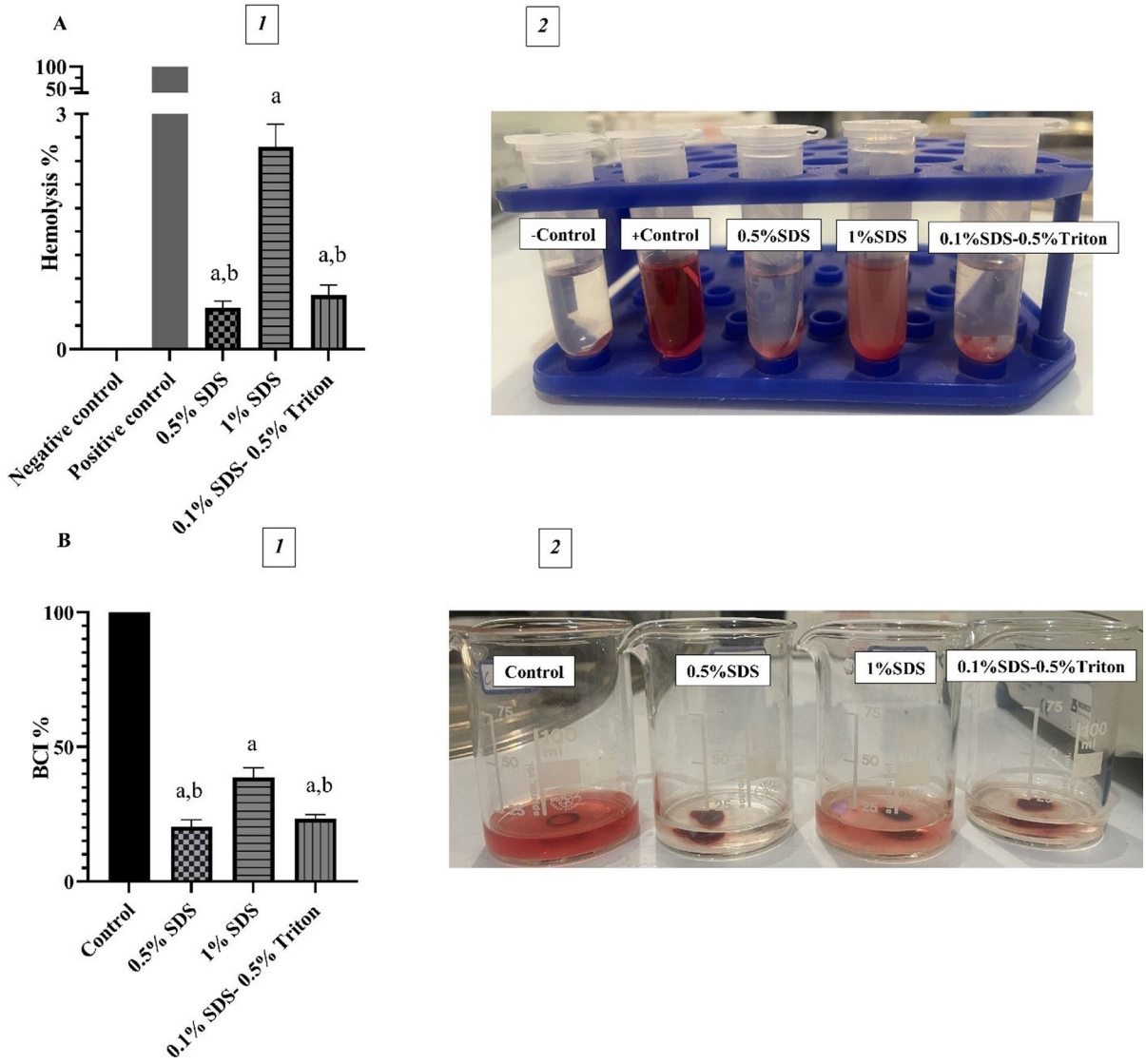

Fig. 3 **A** Hemolysis test: (1) All methods showed significant differences from the positive control group, a: Significant compared to the positive control, b: Significant compared to the 1%SDS group, (2) Hemocompatibility is demonstrated by the clear liquid supernatant in the tubes in the image pertaining to the hemolysis test in DKCs by different techniques, **B** BCI: (1) Comparison of BCI in control and DKCs samples, In the control group there is no scaffold, a: Significant compared to the control group, b: Significant compared to the 1% SDS group (2) Images of the scaffolds after incubation, the data presented are mean ± SD, n = 3

(Dzobo et al. 2018). In addition, decellularization—which separates ECM from native tissues to establish a natural structure—is one of the most promising approaches to tissue and organ regeneration. The ECM can then be repopulated with cells to form a functional tissue or organ, ideally retaining its complex composition, tissue-specific architecture, vascular networks, and biomechanical and biochemical properties (Alizadeh et al. 2022; NOVOTNA et al. 2023).

Decellularization of sheet-like tissues such as the pericardium, the protocol of using 0.1% SDS+trypsin and 1% SDS was optimal compared to the use of TritonX-100 in DNA removal, and these results were in line with our study (Sokol et al. 2020). Effective decellularization of the pig vena cava was

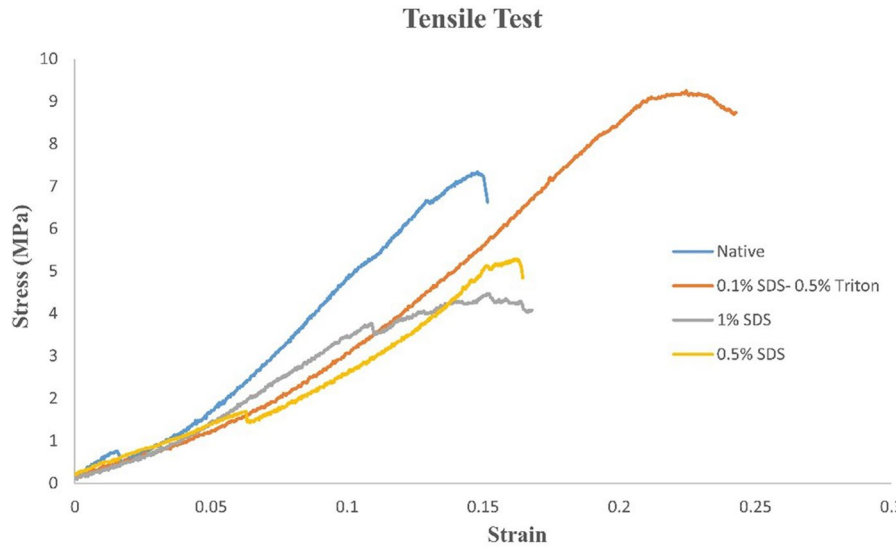

Fig. 4 Mechanical test of the NKC and DKCs tissues

demonstrated by decellularization using SDS, SDC, CHAPS, and TritonX-100 detergents, followed by decellularization utilizing DNase and the perfusion approach in the bioreactor. About 1% of DNA remained in the tissues. On the other hand, treatments based on Triton-X100 have the biggest cellularization impact using HUVECs (Simsa et al. 2018). As the results of our study showed, the percentage of DNA remaining in the tissue in all decellularization methods was reported to be more than 1%, which may be due to the use of DNase in the last stage of decellularization in vascular tissue, which is well DNA has been removed.

Remaining detergents in tissues can affect cell survival and reduce cell proliferation over time. Washing after decellularization steps can be effective in removing detergent and does not reduce cell survival (Khazaei et al. 2023b). Decellularization of chicken skin with different detergents showed a decrease in cell survival over time, which may be due to the lack of washing steps after decellularization (Inci 2022). Considering that in the present study, after decellularization, tissues were washed with distilled water for 24 h, cell survival did not decrease over time. On the other hand, the lower the concentration of SDS in cell removal methods, the higher the cell proliferation was reported.

In histological staining by different methods, the decellularized tissues were analyzed to determine the efficiency of the decellularization methods in terms of the absence of nuclei and to examine the changes of collagen and GAG. As shown by the results in Fig. 2, cells, and cellular components in the decellularized samples were successfully removed after 24 h in the 1% SDS and 0.5% SDS methods, while the lower concentration of SDS+Triton failed to completely decellularize the samples. On the other hand, increasing the concentration of SDS decreased the amount of collagen and GAG in the tissue and to some extent opened the tissue components. Bovine articular cartilage was decellularized using 2.5% SDS solution for 1, 4, and 8 h. The results demonstrated a sharp decline in the tissues' GAG concentration as the decellularization period increased. Thus, the amount of time of decellularization has a direct impact on the levels of collagen and GAG in the tissues in addition to the detergent's concentration (Tavassoli et al. 2015). In a study, porcine fasciocutaneous flaps were decellularized using SDS in three different concentrations (0.1%, 0.2%, and 1%). The results showed that with the increase in detergent concentration, the amount of GAG in the tissue decreases and, in this regard, more DNA is removed from the tissue (Lupon et al. 2024).

Placental decellularization was done by several different methods in a study where only one protocol that was a combination of physical and chemical methods showed a tissue structure similar to normal tissue in SEM and cell adhesion was also well seen on the above scaffold (Sajed et al. 2022). Pericardium decellularized with 1% SDS showed that the detergent partially caused the separation of collagen

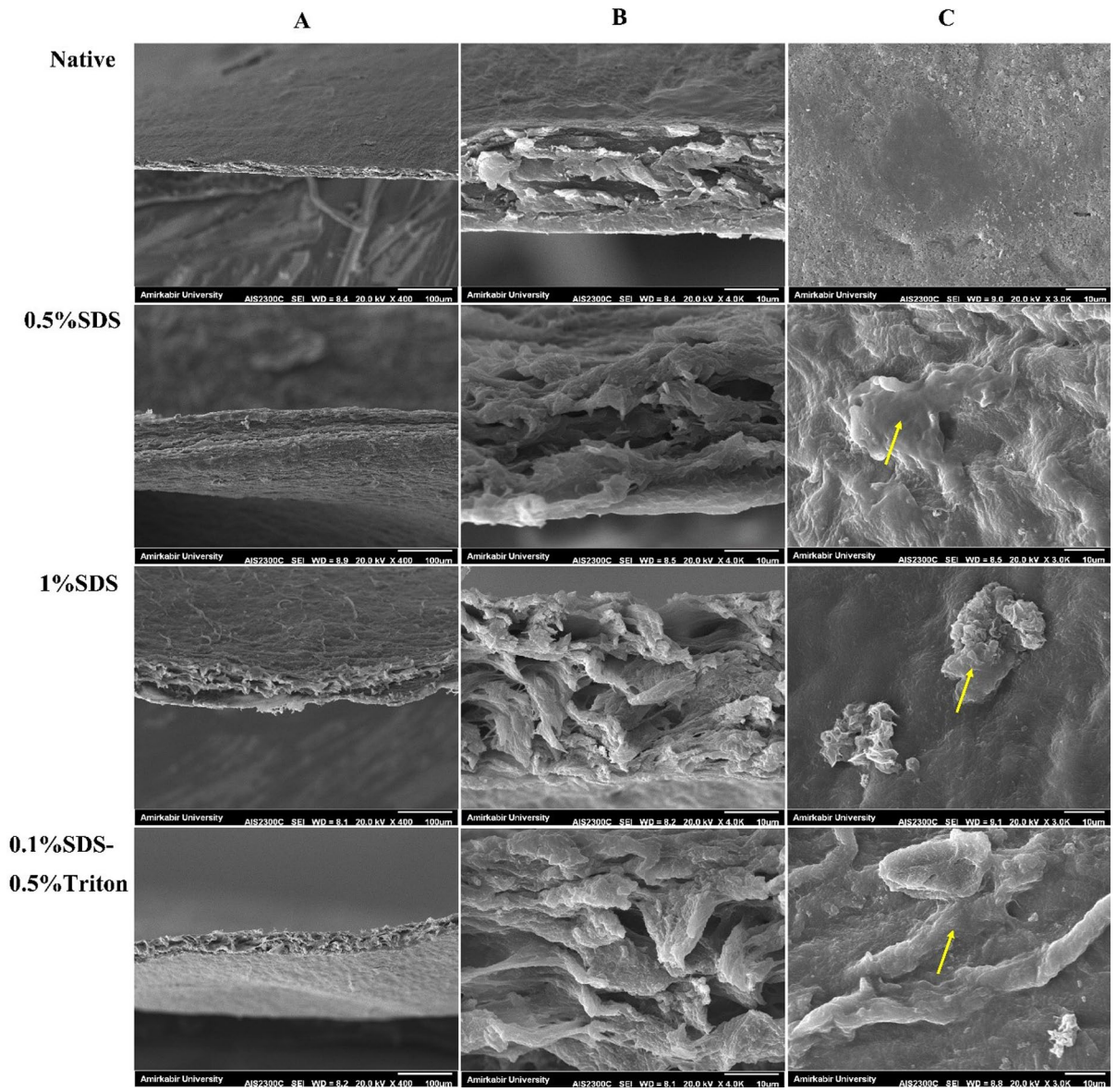

Fig. 5 SEM images, **A** X-400 cross-section of all tissues, **B** X-4.0 K cross-section of all tissues, **C** The cell surface that can be seen in the DKCs samples is cell adhesion with a yellow arrow

fibers (Khazaei et al. 2023b). In the present study, it was also seen that the detergent concentration has a great effect on tissue morphology, which was reported in line with the studies in this field. Foreskin tissue decellularization was compared with two normal methods (1% SDS) and the optimal method (5% SDS, 0.05% trypsin, 0.01% EDTA, 1% Triton-X100). SEM evidence showed that in the optimal method, the collagen fibers have uniform integrity, and the structure of the tissue is well preserved and there is no trace of cells left in the tissue, but in decellularization using the normal method, the SEM was very irregular and the cells were completely not removed from the tissue (Rahmati et al. 2022). In the decellularization of the kidney capsule, it was seen that the structure of the ECM was separated by the 1% SDS method compared to the 0.5% SDS method, but in both methods, the cells were well

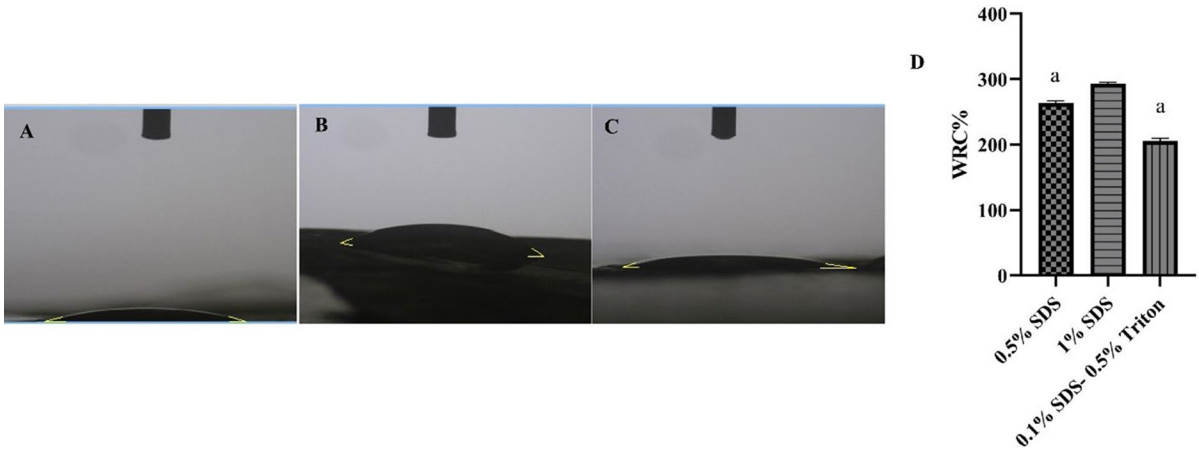

Fig. 6 Contact angle test **A** 0.5% SDS, **B** 1%SDS, **C** 0.1% SDS-0.5% Triton, and **D** WRC test, a: significant compared to the SDS group, the data presented are mean ± SD, n = 3

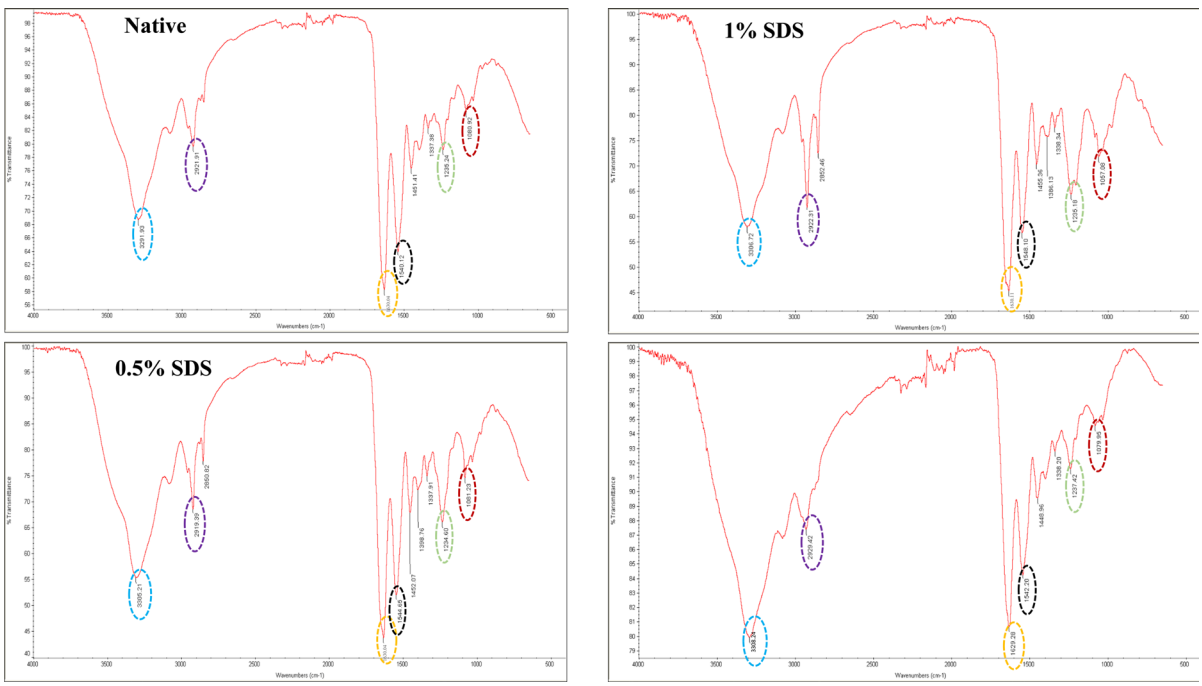

Fig. 7 FTIR spectra of NKC and DKCs by different methods, the same protein range is seen with similar color dashed lines

removed from the tissue, which can be attributed to the thickness tissue.

The blood stability of scaffolds is a good predictor for their use in research because they are in direct contact with blood. Low hemolysis is thought to be a sign of greater hemocompatibility. The American Society for Testing and Materials (ASTM) states that a material is considered non-hemolytic if its hemolysis-causing effect is less than 2% (Sharma et al. 2019). The scaffold prepared by the 1% SDS method reported a hemolysis percentage of more than 2, but in other scaffolds, this number was reported as less than 1%. The combination of 0.5% SDS+0.5% Triton in caprine pericardial decellularization reported

a hemolytic index of 5%, which was higher than our study (Deepak and Babu 2023). Hemostasis capacity is another crucial factor in selecting an appropriate material for wound dressings. Thrombus induction is a crucial therapeutic intervention that can halt bleeding from open wounds and minimize blood loss (Saghebasl et al. 2023). The higher hemostatic ability of 0.5% SDS compared to 1% SDS scaffold may be due to the lower dosage of detergent. There is also a possibility that if we increase the washing time, we can achieve an acceptable percentage of hemostatic degree in the 1% SDS group. The hydrogel obtained from the decellularized pig dermal matrix tissue by chemical and physical methods reported values less than 10% in the BCI test, which indicates good coagulation in the above scaffold (Cai et al. 2021). It seems that the presence of SDS and its concentration has a negative effect on coagulation.

In the native sample, the modulus was high compared to the decellularized samples. Young's modulus was reduced by 0.5%, 1% and 0.5% SDS+0.5% Triton method by 34, 38 and 58%, respectively, compared to native tissue. Therefore, the detergent concentration can reduce the mechanical strength. Since the collagen content of the decellularized tissue is reduced compared to the native tissue, it seems that the mechanical properties of the decellularized tissue are related to the collagen content. Decellularization of pericardial tissue with 1% SDS for 48 h decreased mechanical strength by 46% compared to native tissue (Alizadeh et al. 2021). Therefore, the duration of decellularization can also affect the reduction of mechanical strength.

The decellularized goat small intestine scaffold containing curcumin shows good results in wound healing with its hydrophilic property (Singh et al. 2022). As the results showed in the present study, the highest level of hydrophilicity was reported by the decellularized scaffold with 0.5% SDS. Here too, the detergent concentration on the surface of the scaffold can affect the degree of contact angle. Maybe increasing the washing time can be effective in better removing the detergent from the surface of the scaffold and increase the amount of hydrophilicity. While the highest water retention capacity related to the decellularized scaffold with SDS was 1%. Considering that the higher concentration of the detergent has caused more porosity in the scaffold, as a result, the amount of water retention also increases. In decellularization of tilapia fish, it was seen that the decellularization process increases the wettability of the skin surface, but in the groups in which cross-linking was established, a decrease in hydrophilicity was observed on the surface of the scaffold. Therefore, in addition to decellularization methods, factors such as cross-linkers can also affect the level of hydrophobicity of the scaffold (Liu et al. 2022).

To examine the secondary structure of proteins found in the NKC and DKCs, ATR-FTIR spectroscopy was used (Gupta et al. 2013). In ATR-FTIR of NKC and DKCs, change in the structure of collagen proteins was analyzed using the amide A, B, I, II, and III peaks. Amide infrared radiation absorption spectral amide I (1600–1800 cm^{-1}), II (1470–1570 cm^{-1}), III (1250–1350 cm^{-1}), A (3300–3500 cm^{-1}) (Ji et al. 2020) and B (2919–2950 cm^{-1}) (Rizk and Mostafa 2016) bands are the famous FTIR characterizations of amide. The amide A band is a range of 3300–3500 cm^{-1} corresponding to H-bonded N–H stretching in NKC and DKCs. Bond vibration develops amide A in native (3417 cm^{-1}) and decellularized esophagus (3419 cm^{-1}) (Goyal et al. 2022) was consistent with our study. Amide B has been reported from the tilapia skin 2931 cm^{-1}, indicating the asymmetric stretching vibration of –CH2 which is consistent with the range of Amide B in our study (NKC and DKCs). Studies have revealed a connection between the collagen's triple-helix structure and the amide I, amide II, and amide III bands (Kittiphattanabawon et al. 2010). The C=O stretching vibration was linked to the amide I bands and its absorption bands of NKC, 1% SDS, 0.5% SDS and 0.5% SDS-0.5% Triton appeared at 1630 cm^{-1}, 1630 cm^{-1}, 1630 cm^{-1}, 1629 cm^{-1} respectively. The results of our investigation were consistent with those of amide I measurements made in rat skin, bovine pericardium, and human heart valves (de Campos Vidal and Mello 2011). The amide II peak is connected to the N–H group's rise in hydrogen bonds, and amide II bands are formed by N–H bend and C-N stretching vibrations and have been used to define collagen structure in a way that is analogous to the Amide I band (Haghjooy Javanmard et al. 2016; Benjakul et al. 2010). Amide II was reported in buffalo skin in 1540 cm^{-1}, which was the subject of our study (Rizk and Mostafa 2016). The amide III bands are the grouping of the C-N stretching vibration and the N–H banding vibration (Li et al. 2018). The amide III absorption band of NKC, 1% SDS, 0.5% SDS and 0.5% SDS-0.5% Triton appeared at

1235 cm^{-1}, 1235 cm^{-1}, 1234 cm^{-1}, 1237 cm^{-1} respectively, which are reliable in earlier research (Sun et al. 2017). In native corneal tissue and decellularization with 0.1% Triton, liquid nitrogen, Freeze -thaw, 0.5% Triton and 0.1% SDS, the amount of GAG was reported as 1075 cm^{-1}, 1074 cm^{-1}, 1068 cm^{-1}, 1069 cm^{-1}, 1070 cm^{-1} and 1070 cm^{-1} respectively (Nara et al. 2016). These data or values from our study are in line.

Conclusion

In this study, kidney capsule was decellularized for the first time using combined physical–chemical methods. The above scaffold lost its DNA content after decellularization, and GAG and collagen fibers were largely preserved. Also, it is hydrophilic, hemocompatibility, and biocompatible, and to a large extent it has preserved its mechanical properties like natural tissue. The best decellularization scaffold was introduced with 0.5% SDS. Therefore, it can be proposed as a scaffold that has ECM like natural tissue, for tissue engineering applications.

Acknowledgements The results described in this paper were part of a student thesis. This paper originated from an MD dissertation (research code: 4020769 and 4020857) and with the ethics code IR.KUMS.AEC.1402.261 and IR.KUMS.AEC.1402.239.

Author contributions M.R.K. and R.I. and R.F. and A.B. performed the dissection experiments, data measurement and the statistical analysis, and wrote the first draft of the manuscript. M.K. and L.R. contributed to conception and design of the study. All authors contributed to manuscript revision, read, and approved the submitted version.

Funding This paper was funded research deputy of Kermanshah University of Medical Sciences, Kermanshah, Iran.

Data availability No datasets were generated or analysed during the current study.

Declarations

Conflict of interest No potential conflict of interest was reported by the authors.

References

Alizadeh A, Rezakhani L, Shoa MA, Ghasemi S (2020) Frequency of CD44 positive cells in MKN45 cell line after treatment with docetaxel in two and three-dimensional cell cultures. Tissue Cell 63:101324

Alizadeh M, Rezakhani L, Khodaei M, Soleimannejad M, Alizadeh A (2021) Evaluating the effects of vacuum on the microstructure and biocompatibility of bovine decellularized pericardium. J Tissue Eng Regen Med 15:116–128

Alizadeh M, Rezakhani L, Nooshabadi VT, Alizadeh A (2022) The effect of Scrophularia striata on cell attachment and biocompatibility of decellularized bovine pericardia. Cell Tissue Bank 23:261–269

Benjakul S, Thiansilakul Y, Visessanguan W, Roytrakul S, Kishimura H, Prodpran T, Meesane J (2010) Extraction and characterisation of pepsin-solubilised collagens from the skin of bigeye snapper (Priacanthus tayenus and Priacanthus macracanthus). J Sci Food Agric 90:132–138

Cai D, Chen S, Wu B, Chen J, Tao D, Li Z, Dong Q, Zou Y, Chen Y, Bi C (2021) Construction of multifunctional porcine acellular dermal matrix hydrogel blended with vancomycin for hemorrhage control, antibacterial action, and tissue repair in infected trauma wounds. Mater Today Bio 12:100127

Chandika P, Ko S-C, Gun-Woo Oh, Heo S-Y, Nguyen V-T, Jeon Y-J, Lee B, Jang CH, Kim GeunHyung, Park WS (2015) Fish collagen/alginate/chitooligosaccharides integrated scaffold for skin tissue regeneration application. Int J Biol Macromol 81:504–513

de Campos Vidal B, Mello MLS (2011) Collagen type I amide I band infrared spectroscopy. Micron 42:283–289

Deepak T, Babu AR (2023) Investigation of hemocompatibility and physicochemical properties of acellular caprine pericardium for biomedical applications. J Mater Res 38:1973–1983

Dzobo K, Thomford NE, Senthebane DA, Shipanga H, Rowe A, Dandara C, Motaung KSCM (2018) Advances in regenerative medicine and tissue engineering: innovation and transformation of medicine. Stem Cells Int. https://doi.org/10.1155/2018/2495848

Ehterami A, Masoomikarimi M, Bastami F, Jafarisani M, Alizadeh M, Mehrabi M, Salehi M (2021) Fabrication and characterization of nanofibrous poly(L-Lactic Acid)/chitosan-based scaffold by liquid-liquid phase separation technique for nerve tissue engineering. Mol Biotechnol 63:818–827

Ehterami A, Kolarijani NR, Nazarnezhad S, Alizadeh M, Masoudi A, Salehi M (2022) Peripheral nerve regeneration by thiolated chitosan hydrogel containing taurine: in vitro and in vivo study. J Bioact Compat Polym 37:85–97

Gao S, Guo W, Chen M, Yuan Z, Mingjie Wang Yu, Zhang SL, Xi T, Guo Q (2017) Fabrication and characterization of electrospun nanofibers composed of decellularized meniscus extracellular matrix and polycaprolactone for meniscus tissue engineering. J Mater Chem B 5:2273–2285

Goyal RP, Gangwar AK, Khangembam SD, Yadav VK, Kumar R, Verma RK, Kumar N (2022) Decellularization of caprine esophagus using fruit pericarp extract of Sapindus mukorossi. Cell Tissue Bank 23(1):79–92. https://doi.org/10.1007/s10561-021-09916-w

Guarnieri R, Reda R, Di Nardo D, Miccoli G, Zanza A, Testarelli L (2022) In vitro direct and indirect cytotoxicity comparative analysis of one pre-hydrated versus one dried acellular porcine dermal matrix. Materials 15:1937

Gupta SK, Dinda AK, Potdar PD, Mishra NC (2013) Fabrication and characterization of scaffold from cadaver goat-lung tissue for skin tissue engineering applications. Mater Sci Eng C 33:4032–4038

Haghjooy Javanmard S, Anari J, Zargar Kharazi A, Vatankhah E (2016) In vitro hemocompatibility and cytocompatibility of a three-layered vascular scaffold fabricated by sequential electrospinning of PCL, collagen, and PLLA nanofibers. J Biomater Appl 31:438–449

Inci I (2022) Characterization of decellularized chicken skin as a tissue engineering scaffold. Biotechnol Appl Biochem 69:2257–2266

Ji Y, Yang X, Ji Z, Zhu L, Ma N, Chen D, Jia X, Tang J, Cao Y (2020) 'DFT-calculated IR spectrum amide I, II, and III band contributions of N-methylacetamide fine components. ACS Omega 5:8572–8578

Khazaei MR, Ami Z, Mozafar K, Rezakhani L (2023a) The decellularized calf testis: introducing suitable scaffolds for spermatogenesis studies. Int J Fertil Steril 18(1):32

Khazaei M, Alizadeh M, Rezakhani L (2023b) Resveratrol-loaded decellularized ovine pericardium: ECM introduced for tissue engineering. Biotechnol Appl Biochem 71(2):387–401. https://doi.org/10.1002/bab.2547

Kim B-S, Kim J-U, So K-H, Hwang NS (2021) Supercritical fluid-based decellularization technologies for regenerative medicine applications. Macromol Biosci 21:2100160

Kittiphattanabawon P, Benjakul S, Visessanguan W, Shahidi F (2010) Isolation and properties of acid-and pepsin-soluble collagen from the skin of blacktip shark (*Carcharhinus limbatus*). Eur Food Res Technol 230:475–483

Lee JS, Choi YS, Lee JS, Jeon EJ, An S, Lee MS, Yang HS, Cho S-W (2022) Mechanically-reinforced and highly adhesive decellularized tissue-derived hydrogel for efficient tissue repair. Chem Eng J 427:130926

Lee JS, Choi YS, Cho SW (2018) Decellularized tissue matrix for stem cell and tissue engineering. Biomimetic Medical Materials: From Nanotechnology to 3D Bioprinting, 161–80

Li L-Y, Yu-Qin Zhao Yu, He C-F, Wang B (2018) Physicochemical and antioxidant properties of acid-and pepsin-soluble collagens from the scales of miiuy croaker (*Miichthys miiuy*). Mar Drugs 16:394

Liu Z, Ming-Zhao Yu, Peng H, Liu R-T, Lim T, Zhang C-Q, Zhu Z-Z, Wei X-J (2022) Decellularized tilapia fish skin: a novel candidate for tendon tissue engineering. Mater Today Bio 17:100488

Lupon E, Acun A, Taveau CB, Oganesyan R, Lancia HH, Andrews AR, Randolph MA, Cetrulo Jr CL, Lellouch AG, Uygun BE (2024) Optimized decellularization of a porcine fasciocutaneaous flap. Bioengineering 11:321

Nara S, Chameettachal S, Midha S, Murab S, Ghosh S (2016) Preservation of biomacromolecular composition and ultrastructure of a decellularized cornea using a perfusion bioreactor. RSC Adv 6:2225–2240

Neishabouri A, Khaboushan AS, Daghigh F, Kajbafzadeh A-M, Zolbin MM (2022) Decellularization in tissue engineering and regenerative medicine: evaluation, modification, and application methods. Front Bioeng Biotechnol 10:805299

Novotna O, Novakova ZV, Galfiova P, Lorencova M, Klein M, Žiaran S, Kuniakova M (2023) Decellularization techniques of human foreskin for tissue engineering application. Physiol Res 72(Suppl 3):S287

Prasertsung I, Kanokpanont S, Bunaprasert T, Thanakit V, Damrongsakkul S (2008) 'Development of acellular dermis from porcine skin using periodic pressurized technique. J Biomed Mater Res Part B Appl Biomater off J Soc Biomater Jpn Soc Biomater Aust Soc Biomater Korean Soc Biomater 85:210–219

Rahmati S, Jalili A, Dehkordi MB, Przedborski M (2022) An effective method for decellularization of human foreskin: implications for skin regeneration in small wounds. Cell J 24:506

Rizk MA, Mostafa NY (2016) Extraction and characterization of collagen from buffalo skin for biomedical applications. Orient J Chem 32:1601

Saghebasl S, Amini H, Nobakht A, Haiaty S, Bagheri HS, Hasanpour P, Milani M, Saghati S, Naturi O, Farhadi M (2023) Polyurethane-based nanofibrous mat containing porphyrin with photosensitivity and bactericidal properties can promote cutaneous tissue healing in rats. J Nanobiotechnol 21:313

Sajed R, Zarnani A-H, Madjd Z, Arefi S, Bolouri MR, Vafaei S, Samadikuchaksaraei A, Gholipourmalekabadi M, Haghighipour N, Ghods R (2022) Introduction of an efficient method for placenta decellularization with high potential to preserve ultrastructure and support cell attachment. Artif Organs 46:375–386

Sharifi M, Kheradmandi R, Salehi M, Alizadeh M, Ten Hagen TLM, Falahati M (2022) Criteria, challenges, and opportunities for acellularized allogeneic/xenogeneic bone grafts in bone repairing. ACS Biomater Sci Eng 8:3199–3219

Sharma S, Laxmi Swetha K, Roy A (2019) Chitosan-Chondroitin sulfate based polyelectrolyte complex for effective management of chronic wounds. Int J Biol Macromol 132:97–108

Simsa R, Padma AM, Heher P, Hellström M, Teuschl A, Jenndahl L, Bergh N, Fogelstrand P (2018) Systematic in vitro comparison of decellularization protocols for blood vessels. PLoS ONE 13:e0209269

Singh H, Purohit SD, Bhaskar R, Yadav I, Bhushan S, Gupta MK, Mishra NC (2022) Curcumin in decellularized goat small intestine submucosa for wound healing and skin tissue engineering. J Biomed Mater Res B Appl Biomater 110:210–219

Sizeland KH, Hofman KA, Hallett IC, Martin DE, Potgieter J, Kirby NM, Hawley A, Mudie ST, Ryan TM, Haverkamp RG (2018) Nanostructure of electrospun collagen: do electrospun collagen fibers form native structures? Materialia 3:90–96

Sokol AA, Grekov DA, Yemets GI, Yu Galkin A, Shchotkina NV, Dovghaliuk AA, Telehuzova OV, Rudenko NM, Romaniuk OM, Yemets IM (2020) Comparison of bovine pericardium decellularization protocols for production of biomaterial for cardiac surgery. Biopolym Cell 36:392

Sun L, Hou Hu, Li B, Zhang Y (2017) Characterization of acid-and pepsin-soluble collagen extracted from the skin of Nile tilapia (*Oreochromis niloticus*). Int J Biol Macromol 99:8–14

Tavassoli A, Matin MM, Niaki MA, Mahdavi-Shahri N, Shahabipour F (2015) Mesenchymal stem cells can survive

on the extracellular matrix-derived decellularized bovine articular cartilage scaffold. Iran J Basic Med Sci 18:1221

Wang J, Zhao Li, Zhang A, Huang Y, Tavakoli J, Tang Y (2018) Novel bacterial cellulose/gelatin hydrogels as 3D scaffolds for tumor cell culture. Polymers 10:581

Zhang X, Chen Xi, Hong H, Rubei Hu, Liu J, Liu C (2022) Decellularized extracellular matrix scaffolds: Recent trends and emerging strategies in tissue engineering. Bioact Mater 10:15–31